CHEMICAL ENGINEERING TRANSACTIONS
VOL. 60, 2017
A publication of AIDIC
The Italian Association of Chemical Engineering
Online at www.aidic.it/cet
Guest Editors: Luca Di Palma, Elisabetta Petrucci, Marco Stoller

ISBN978-88-95608- 50-1; **ISSN** 2283-9216
DOI: 10.3303/CET1760033

Pore-Scale Simulations of Particle Transport for Groundwater Remediation: the Effect of Gravitational Settling

Eleonora Crevacore*[a], Gianluca Boccardo[b], Alfio Grillo[a], Daniele L. Marchisio[c], Rajandrea Sethi[d]

[a]DISMA "G.L. Lagrange", Politecnico di Torino, C.so Duca degli Abruzzi 24, 10129 Torino, Italy
[b]School of Mechanical Engineering, Tel Aviv University, Tel Aviv, 69978, Israel
[c]DISAT, Politecnico di Torino, C.so Duca degli Abruzzi 24, 10129 Torino, Italy
[d]DIATI, Politecnico di Torino, C.so Duca degli Abruzzi 24, 10129 Torino, Italy
eleonora.crevacore@polito.it

In this work, we investigate particle deposition efficiency in porous media by way of pore-scale computational fluid dynamics simulations. First, we show how to employ a novel methodology of algorithmic generation of porous media to build the computational domain for our simulations, representing a realistic random packing of monodisperse spheres. Then, we focus on the effect of gravitational settling on particle deposition, comparing our results with the well-known simplified theoretical laws, showing how pore-scale numerical experiments can improve the prediction accuracy of these laws but, most of all, help gain fundamental insights in the physical mechanisms at work.

1. Introduction

In recent years, access to clean water has become one of the most urgent environmental issues, and is relevant on a global scale. Remediation of groundwater systems from anthropogenic contamination is thus the focus of many studies. Among these, a very promising line of research is the injection of micro- and nanoscopic zero-valent iron (ZVI) in contaminated sites (Muradova et al, 2016), as iron particles have been shown to be particularly effective in the deactivation and removal of several species of contaminants, especially in the particularly problematic dense non-aqueous phase liquids (DNAPL) category.
In order to engineer an effective intervention in contaminated sites, full knowledge of the nature of transport of ZVI particles is paramount. To this end, computational fluid dynamics studies offer an exceptional tool to predict the dispersion and length of migration of the injected particles, before their deposition on the solid matrix of the porous medium. CFD is indeed a consolidated methodology for the study of the fluid dynamic behavior in both arranged and random packed systems (Haddadi et al., 2016, Mitrichev et al., 2016), and it provide a precise assessment of pore-scale phenomena; this enhanced knowledge is then transported, via appropriate up-scaling procedures, to readily employable macro-scale models (Pereira et al., 2014).
The problem of colloidal particle deposition has often been tackled from simplified theoretical perspectives (Levich, 1962, Yao, 1971, Rajagopalan and Tien, 1976). While the classical approach allows the detailed study of all the interactions involved in deposition processes (namely Brownian deposition, steric interception, and gravitational settling), the geometric model underneath is the single spherical collector, which practically conceals (or better, does not allow to take into account) the important role played by the realistic structure of the porous medium. Thus, neither the pore-scale effects of grain shape and size distribution, nor the meso-scale effect of geometric heterogeneity can be explored with this traditional approach. Nevertheless, recent works have tried to improve this description with CFD simulations on simplified models or small random packings (Ma et al., 2010, Johnson and Hilpert, 2013) to better represent the solid matrix at the pore scale.
The aim of the present contribution is to put forward some preliminary results that help to advance this line of research. This study thus considers three different realizations of realistic random packings in order to explore particle transport under the simultaneous action of Brownian deposition and gravitational settling.

Please cite this article as: Crevacore E., Boccardo G., Grillo A., Marchisio D., Sethi R., 2017, Pore-scale simulations of particle transport for groundwater remediation: the effect of gravitational settling, Chemical Engineering Transactions, 60, 193-198 DOI: 10.3303/CET1760033

We used the open-source code OpenFOAM to perform CFD simulations. First, the fluid flow field is solved in steady-state conditions in laminar regime, then particle transport and deposition are studied solving the classical advection-diffusion equation, under a broad range of operating conditions.
Finally, corrected constitutive equations for the prediction of particle deposition due to Brownian diffusion and gravitational settling are formulated.

2. Theoretical background

In this work we will approach the study of fluid flow and colloid transport at the pore-scale, identifying and solving in the CFD code the relevant transport equations.
A number of simplifying hypotheses have been employed. Since the main application in sight of this study is in the field of groundwater remediation, the fluid has been considered Newtonian and incompressible; moreover, we limit this study to the saturated zone (i.e., the inter-granular zone is entirely occupied by water). Hence, the relevant transport equations for fluid flow are the stationary Navier-Stokes equation and the mass balance law, which read:

$$\rho\left(\nabla \boldsymbol{U}_f\right)\boldsymbol{U}_f = -\nabla p + \mu\Delta\boldsymbol{U}_f \,, \tag{1}$$

$$\nabla \cdot \boldsymbol{U}_f = 0 \,, \tag{2}$$

where ρ is the fluid density (kg m^{-3}), $\boldsymbol{U}_f$ is the fluid velocity (m s^{-1}), p is the pressure (kg m^{-1} s^{-2}) and μ is the fluid dynamic viscosity (kg m^{-1} s^{-1}). As is customary for the solution of continuum fluid transport problems, the boundary condition $\boldsymbol{U}_f = \boldsymbol{0}$ is imposed on the surface of the grains, while the driving force for the motion of the fluid results from setting a pressure difference between two opposing sides of the domain. Note that the applied pressure difference represents the pressure head.
Colloidal particles are modeled in an Eulerian framework, solving for their concentration. The one-way coupling hypothesis is employed, stating that the flowing fluid (and external forces) will affect the motion of the particles, but not the vice-versa. In this case, the reference pore-scale description of the solute concentration transport is the advection-diffusion equation, which reads:

$$\frac{\partial \mathrm{c}}{\partial \mathrm{t}} + \boldsymbol{U}_p \cdot \nabla c = D\Delta c \,, \tag{3}$$

where c is the particle concentration (kg m^{-3}) and $\boldsymbol{U}_p$ is the particle velocity (m s^{-1}); D is the molecular diffusion coefficient of the particles (m^2 s^{-1}), which can be estimated with the aid of the Stokes-Einstein equation:

$$D = \frac{\kappa_B T}{6\pi\mu r_p} \,, \tag{4}$$

where κ_B is the Boltzmann constant, T is the temperature (K) and r_p is the particle radius (m). We emphasize that $\boldsymbol{U}_p$ is assumed here to be solenoidal. In the simplest case, $\boldsymbol{U}_p$ coincides with the fluid velocity $\boldsymbol{U}_f$. However, when sedimentation has to be considered, $\boldsymbol{U}_p$ is implemented as the sum of the fluid velocity and the particles' settling velocity, the latter defined as:

$$\boldsymbol{U}_{settl} = \frac{2}{9}\frac{(\rho_p - \rho)\boldsymbol{g}r_p^2}{\mu} \,, \tag{5}$$

where ρ_p is the density (kg m^{-3}) of the transported particles. To obtain the steady-state solution for the colloidal deposition problem, a boundary condition of constant unitary concentration on the domain inlet was set, while the concentration at the surface of the grains was set equal to zero. This last condition represents the well-known "perfect sink condition" (Tien and Ramarao, 2011), which gives a good description of the conditions in a filtration process at its early stages (i.e., when particle straining and filter loading are minimal) and when physico-chemical conditions are favorable to colloidal attachment.

2.1 Colloidal deposition

Under the perfect sink condition, colloidal deposition has been widely (theoretically and numerically) studied (Levich, 1962, Yao et al., 1971, Elimelech et al., 1995, Yao et al., 1971, Nelson and Ginn, 2005, Ma and Johnson, 2009), and the most used description of the process sees it happening in two phases. First, the transport of the particles from the bulk of the fluid to the collector surface is quantified by the deposition efficiency η_0, which is defined as:

$$\eta_0 = \frac{\textit{flux of particles reaching the collector}}{q\frac{C_0 \pi d_g^2}{4}}\ , \tag{6}$$

where the denominator represents the flux of particles moving towards the collector by advection; q is the superficial (Darcyan) velocity (m s^{-1}), C_0 is the inlet concentration (kg m-3) and d_g is the grain diameter (m). Secondly, the attachment of the particles to the surface of the grains, depending on the balance between grains-collector repulsive and attractive forces, is quantified by the attachment efficiency α, which can assume values between 0 and 1. Then, the total colloidal deposition efficiency η can be expressed as the product between these two terms, i.e. $\eta = \alpha\eta_0$. As mentioned earlier, we explore the case of favorable clean-bed filtration, hence $\alpha = 1$. This method can nonetheless be successfully employed also in cases where $0 < \alpha < 1$, see for example (Boccardo et al., 2017).

The deposition efficiency η_0 depends on the contribution of three different mechanisms, namely Brownian diffusion, steric interception, and gravitational settling. Prieve and Ruckenstein (1974), positing an additive synergy between them, wrote $\eta_0 = \eta_B+\eta_I+\eta_G$. The first summand, relevant for sub-micron sized particles, brings particles in contact with the collector via their random motion due to molecular diffusion. Interception is a steric effect which causes particles to collide with the collector due to their finite dimension, and is stronger the larger their size with respect to the solid grains. Lastly, gravitational settling takes into account the additional force moving colloids towards the collectors due to gravity.

While in our earlier numerical works we investigated Brownian deposition in a variety of porous media models (Boccardo et al., 2014, Crevacore et al. 2016 (a), Boccardo et al., 2017), the purpose of this work is to explore the effect of gravity on particle deposition. In the formulation by Yao et al. (1971) of the three mechanism efficiencies, the influence of gravity was described as:

$$\eta_G = {U_{settl}}/{q} = N_G\ , \tag{7}$$

where U_{settl} is the magnitude of the particle settling velocity, already written in Eq(5), and the ratio between this velocity and the fluid superficial velocity takes the name of gravity number, N_G.

In this work we aim to show that Eq(7), while constituting an useful indication, usually fails to take into account many important features of the system under investigation. Furthermore, we will show how detailed pore-scale simulations can correct and improve the estimation of η_G.

3. Numerical details

In this work, the porous medium structure is described with random packing arrangements of mono-dispersed spherical grains. The geometrical model is obtained by using Blender, an open-source software for digital graphics, following the procedure sketched in Figure 1. Grains are packed within a cylindrical container. To obtain the geometries presented in this work, 7,800 grains having a diameter of d_g=100 μm have been packed in a container 1.86 mm high and with cross-section diameter of 2.15 mm. Grains are at first located above the container, displaced on grids on different levels. A small perturbation is added to the grains position, to ensure randomness of the final grains displacement. Grains are then free to fall under the effect of gravity, which is the only active force, while the friction exerted by the surrounding domain (air) is neglected. Grains are treated as non-deformable bodies. Hence, they cannot compenetrate each other and the only interactions considered are instantaneous collisions and sliding. These interactions are respectively governed by the restitution coefficient (i.e. the ratio of the kinetic energy before and after collision) and the friction factor (depending on the roughness of the grains), both chosen such that the resulting bulk porosity lies in an admissible range for realistic porous media (Boccardo et al., 2015, Augier et al., 2010). The system reaches its mechanical equilibrium when the forces balance each other out and grains are thus fixed.

To be used in CFD simulations, different cubic samples were then extracted from the bulk of the cylindrical container, being aware that wall effects (due to the presence of the container itself) are negligible for distances (from the cylindrical wall inwards) greater than ~5d_g. Three different cubic cuts were then extracted from three different geometric realizations, all composed of ~350 grains, with length L of the side of the cube being equal to 700 μm.

For the CFD simulations, the main axes of the cubic domain are aligned with a Cartesian frame of reference, and the two faces orthogonal to the x-axis are identified as inlet and outlet.

The OpenFOAM software (version 3.0.1) is used for the meshing process as well as for the solution of Eqs(1-3). A body-fitted mesh is adopted, where a greater level of refinement is prescribed close to the grain surface to guarantee a satisfactory description of the flow and concentration boundary layers. In particular, the meshing strategy used is the one described in previous works (Crevacore et al., 2016 (a), Crevacore et al., 2016 (b), Boccardo et al., 2015), where mesh-independence analyses were also presented.

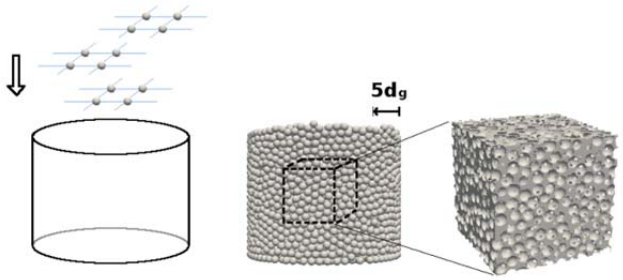

Figure 1:Scheme of the random packing generation with monodispersed grains.

Table 1: Operating conditions

Re	d_p (nm)	U_{settl} (m s^{-1})	N_G	Pe
2.58 10^{-4}	897	2.85 10^{-6}	0.35	588
3.33 10^{-4}	897	2.85 10^{-6}	0.30	686
4.00 10^{-4}	897	2.85 10^{-6}	0.25	823
5.00 10^{-4}	897	2.85 10^{-6}	0.20	1,026
6.70 10^{-4}	897	2.85 10^{-6}	0.15	1,374
1.00 10^{-3}	897	2.85 10^{-6}	0.10	2,060
1.00 10^{-4}	634	1.43 10^{-6}	0.05	1,456

The simpleFoam solver is used to solve the fluid flow equations Eqs(1-2), while scalarTransportFoam was used to solve the particle transport and deposition problem of Eq(3).
For the flow field simulations, the fluid considered is water at room temperature. The applied pressure drop is such that the resulting Reynolds numbers (Re = $\rho d_g q/\mu$) span falls in the laminar regime. Velocities are thus compatible with environmental applications. These very same operating conditions are used also for the simulation of particle Brownian deposition and gravitational settling, as reported in Table 1, where the Péclet number reads Pe = $U_f L/D$, given L the domain length (m) in the main flow direction (in our case the x-axis).
As we aim to model nZVI particles, ρ_p is chosen equal to 7,874 kg m^{-3}.
In order to obtain the values of η_G, for each operating condition two different simulations are run. First, only the Brownian diffusion mechanism is present (via the diffusive term in Eq(3)) and the particle velocity is set equal to that of the fluid: from this simulations the value of $\eta_0 = \eta_B$ is obtained. Then, parallel simulations are performed, adding the effect of gravitational settling. This is done by setting the particle velocity in Eq(3) equal to $\boldsymbol{U_p} = \boldsymbol{U_f}+\boldsymbol{U_{settl}}$, thus considering the effect of the gravitational pull on the denser particles; again, a value of η_0 was extracted. It has to be noted that, generally, we considered the gravitational pull to act in a direction orthogonal to the main fluid flow direction, in order to represent the situation more commonly encountered in colloidal dispersion transport in sub-surface water. In order to expand on the classical representation of this phenomenon, we also consider the case of gravity acting parallel to the flow direction. The comparison between the two cases will be expanded upon in the next Results section. From these last runs, remembering the additive relation between the three mechanisms, η_G is obtained as $\eta_G = \eta_0-\eta_B$ (since we do not model the effect of steric interception in our simulations).
For both pure-Brownian and sedimentation runs, the total deposition efficiency η_0 is evaluated following the packed-bed filtration equation (Logan et al., 1995):

$$\eta_0 = \frac{ln\left(\frac{C_{out}}{C_0}\right)}{\frac{3(1-\varepsilon)L}{2\ \varepsilon\ d_g}}, \tag{8}$$

where C_{out} and C_0 are the outlet an inlet concentrations (kg m^{-3}) and ε is the medium porosity.

4. Results

As mentioned, for each of the operating conditions found in Table 1, simulations with only Brownian deposition are run and compared with simulations where both Brownian and sedimentation mechanisms are present. The difference between these two cases is made evident in Figure 2, which shows the concentration contour plots in a central section of the domain, parallel to the fluid flow direction, in one of the geometries explored (Pe = 588). The great impact of gravity deposition is readily apparent.

Then, to compare our numerical results with the theoretical law from Yao et al. (1971), the sedimentation deposition efficiency is compared with the gravity number N_G (the only parameter influencing η_G in the theoretical description of this process). The behavior of η_G as a function of N_G is shown in Figure 3 (left), for the three geometrical realizations considered.

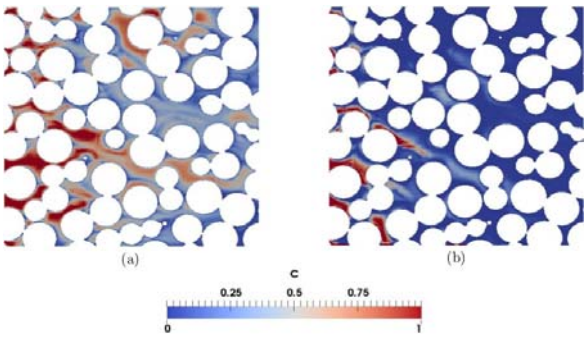

Figure 2: Contour plots of (a) Brownian versus (b) Brownian + sedimentation deposition mechanisms.

Considering all the data in Figure 3 (left) as an aggregate, we can write an equation for a single η_G - N_G relationship, which reads:

$$\eta_G = 0.61 N_G - 0.03 \,, \tag{9}$$

which differs from the Yao's theoretical law, $\eta_G = N_G$, especially in the range of very low gravity numbers, where the behavior appears to be non-linear. Moreover, both the differences of the CFD results compared with the theoretical law and among the three cases themselves could be explained by the inadequacy of the gravity number to provide a full description of the sedimentation mechanism. Indeed, this evaluation of η_G via only the N_G parameter lacks the contribution of (for example) grain diameter and porous media tortuosity.
Another feature of great influence in the study of gravitational settling is the orientation of the gravity force with respect to the main flow direction. The theoretical law was written based on a model where the two directions were thought of as orthogonal to each other; as such, it fails to take into account all other cases. To perform a preliminary exploration of this issue, we conducted another set of simulations, and compared the difference in deposition efficiency between the case of gravity orthogonal and parallel to the fluid direction. The results are shown in Figure 3 (right).
Considering the two result sets independently, we can write two equations for the two cases, which read:

$$\eta_G = 0.71 N_G - 0.04 \,, \tag{10}$$

$$\eta_G = 0.33 N_G - 0.003 \,, \tag{11}$$

both again quite different from the theoretical predictions. Now, in the case of the parallel-acting gravity the colloidal particles have a smaller residence time in the domain with respect to the orthogonal case, as the magnitude of the particle velocity is greater. Thus, lower values of deposition efficiency are observed in this case, identifying in the angle between gravity and the flow direction another parameter of great impact on the estimation of total deposition efficiency.

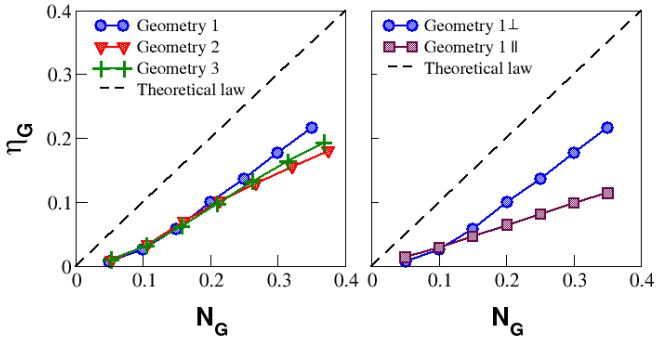

Figure 3: Deposition efficiency by sedimentation versus gravity number. On the left: three different geometric realizations, with gravity acting orthogonally to the fluid flow direction. On the right: difference between the gravity vector being orthogonal or parallel to the main flow direction.

5. Conclusions

In this work, an important physical insight has been gained by clearly highlighting a point of failure of the classical laws for the prediction of deposition efficiency in the case of gravitational settling. While offering a correction to the coefficients in the original formulation, these results clearly indicate how the classical laws do not offer a good description of the underlying phenomena. As an example, it has been shown that, when ignoring the very noticeable effect of gravity orientation with respect to the fluid direction, salient differences emerge looking for predictions of deposition efficiency. Consequently, these differences are relevant when trying to apply the same theoretical law to different scenarios, such as subsurface contaminant transport with respect to industrial water filtration.

Acknowledgments

This work has been supported in part by the Politecnico di Torino (Italy), in part by the Fondazione Cassa di Risparmio di Torino (Italy), through the “La Ricerca dei Talenti” (“HR Excellence in Research”) programme.
We acknowledge the CINECA award under the ISCRA initiative and HPC@POLITO (http://www.hpc.polito.it) for the availability of high performance computing resources and support.
We would also like to acknowledge the valuable contribution of Valeria Bizzarro.

Reference

Augier, F., Idoux, F., Delenne, J.Y., 2010, Numerical simulations of transfer and transport properties inside packed beds of spherical particles. Chemical Engineering Science, 65(3), 1055-1064.
Boccardo, G., Augier, F., Haroun, Y., Ferre, D. and Marchisio, D.L., 2015, Validation of a novel open-source work-flow for the simulation of packed-bed reactors. Chemical Engineering Journal, 279, 809-820.
Boccardo, G., Crevacore, E., Sethi, R. and Icardi, M., 2017, A robust upscaling of the effective particle deposition rate in porous media. arXiv preprint arXiv:1702.04527.
Boccardo, G., Marchisio, D.L. and Sethi, R., 2014, Microscale simulation of particle deposition in porous media. Journal of colloid and interface science, 417, 227-237.
Crevacore, E., Boccardo, G., Marchisio, D. and Sethi, R., 2016, Microscale colloidal transport simulations for groundwater remediation. Chemical Engineering Transactions, 47, 271-276.
Crevacore, E., Tosco, T., Sethi, R., Boccardo, G. and Marchisio, D.L., 2016, Recirculation zones induce non-Fickian transport in three-dimensional periodic porous media. Physical Review E, 94(5), 053118.
Elimelech, M., Gregory, J. and Jia, X., 1995, Particle deposition and aggregation: measurement, modelling and simulation. Butterworth-Heinemann, MA.
Haddadi, B., Jordan, C., Norouzi, H.R., Harasek, M., 2016, Investigation of the pressure drop of random packed bed adsorbers. Chemical Engineering Transactions, 52.
Johnson, W.P. and Hilpert, M., 2013, Upscaling colloid transport and retention under unfavorable conditions: Linking mass transfer to pore and grain topology. Water Resources Research, 49(9), 5328-5341.
Levich, V. G., 1962, Physicochemical hydrodynamics, Prentice-Hall Englewood Cliffs, NJ.
Logan, B.E., Jewett, D.G., Arnold, R.G., Bouwer, E.J. and O'Melia, C.R., 1995, Clarification of clean-bed filtration models. Journal of Environmental Engineering,121(12), 869-873.
Ma, H. and Johnson, W.P., 2009, Colloid retention in porous media of various porosities: Predictions by the hemispheres-in-cell model. Langmuir, 26(3), 1680-1687.
Ma, H., Pedel, J., Fife, P. and Johnson, W.P., 2010, Hemispheres-in-Cell Geometry to Predict Colloid Deposition in Porous Media. Environmental Science & Technology, 44(11), 4383-4383.
Mitrichev, I.I., Jhensa, A.V., Koltsova, E.M., 2016, On the dependence of flow properties on porosity in an open-cell foam. Chemical Engineering Transactions, 52.
Muradova, G., Gadjieva, S., Di Palma, L., Vilardi, G., 2016, Nitrates removal by bimetallic nanoparticles in water. Chemical Engineering Transactions, 47, 205-210.
Nelson, K.E. and Ginn, T.R., 2005, Colloid filtration theory and the Happel sphere-in-cell model revisited with direct numerical simulation of colloids. Langmuir, 21(6), 2173-2184.
Pereira, M.F., Pozza, S.A., Timóteo, V.S., 2014, Numerical methods for the evaluation of pollutant dispersion based on advection-diffusion equation. Chemical Engineering Transactions, 39.
Prieve, D.C. and Ruckenstein, E., 1974, Effect of London forces upon the rate of deposition of Brownian particles. AIChE Journal, 20(6), 1178-1187.
Rajagopalan, R. and Tien, C., 1976, Trajectory analysis of deep-bed filtration with the sphere□in□cell porous media model. AIChE Journal, 22(3), 523-533.
Tien, C. and Ramarao, B.V., 2011. Granular filtration of aerosols and hydrosols. Elsevier.
Yao, K.M., Habibian, M.T. & O'Melia, C.R., 1971, Water and waste water filtration. Concepts and applications. Environmental science & technology, 5, 1105-1112.